GMe Forum 2008

Abstracts of the Poster Presentations

Vienna University of Technology
November 13 and 14, 2008

Society for Micro- and Nanoelectronics
Vienna, 2008

Society for Micro- and Nanoelectronics
c/o Institute of Sensor and Actuator Systems
Vienna University of Technology
Gusshausstrasse 27–29/366
A-1040 Vienna, Austria

Photonics and Optoelectronics:

1. Ch. Deutsch, A. Benz, G. Fasching, K. Unterrainer, A. M. Andrews, P. Klang, W. Schrenk, G. Strasser, *Performance of Phonon Depopulated Terahertz Quantum Cascade Lasers*
2. A. Benz, Ch. Deutsch, G. Fasching, K. Unterrainer, A.M. Andrews, P. Klang, W. Schrenk, G. Strasser, *Photonic Crystal Frequency Control in Terahertz Lasers*
3. Gang Chen, V. Lavchiev, F. Schäffler, G. Bauer, W. Jantsch, *Fabrication of Ordered Ge Quantum Island Arrays on Prepatterned SOI Platform for Waveguide Photodetectors and Emitters*
4. R. Seyrkammer, J. Roither , M.V. Kovalenko, W. Heiss, *Highly Efficient (Infra)-Red-Conversion of InGaN Light Emitting Diodes by Nanocrystals, Enhanced by Color Selective Mirrors*

Nanostructures and Quantum Devices:

5. S. Kriechbaumer, T. Schwarzl, H. Groiss, W. Heiss, T. Wojtowicz, G. Springholz, *Widely Tunable and Intense Mid-Infrared PL Emission from Epitaxial Pb(Sr)Te Quantum Dots in a CdTe Matrix*
6. M. Bergmair, K. Hingerl, *Coupled Surface States in Thin, Frequency Dependent Layers*
7. T. Gebhard, D. Alvarenga, P.L. Souza, P.S.S. Guimarães, K. Unterrainer, M.P. Pires, G.S. Vieira, J.M. Villas-Boas, N. Studart, *Intraband Auger Effect in InAs/InGaAlAs/InP Quantum Dot Structures*
8. J. Smoliner, W. Brezna, A.M. Andrews, G. Strasser, *Quantitative Scanning Capacitance Microscopy on Buried InAs Quantum Dots*
9. M. Keplinger, D. Kriegner, B. Mandl, J. Stangl, V. Chamard, E. Wintersberger, R.T. Lechner, D. Hufnagl, G. Bauer, *Characterization of Nanowires*
10. P. Klang, H. Detz, A.M. Andrews, B. Basnar, W. Schrenk, A. Lugstein, G. Strasser, *Low Dimensional Nanostructures Grown by Molecular Beam Epitaxy*
11. G. Pozzovivo, J. Kuzmik, S. Abermann, C. Ostermaier, J.-F. Carlin, M. Gonschorek, E. Feltin, J. Liday, N. Grandjean, E. Bertagnolli, G. Strasser, D. Pogany, *Recent Improvements on InAlN/GaN MOS-HEMTs*
12. P. Rauter, T. Fromherz, G. Bauer, N.Q. Vinh, G. Mussler, D. Grützmacher, *Voltage Tunability of Intersubband Lifetimes in SiGe Quantum Well Structures*
13. D.G. Matei, B. Sandujav, G. Chen, F. Schäffler, G. Springholz, *In-situ STM Studies of Ge Growth on Stripe-Patterned Si-(001)*

Novel Materials:

14. O. Bethge, S. Abermann, C. Henkel, C. Straif, E. Bertagnolli, *Atomic Layer Deposition of High-k Gate Dielectrics on Germanium and Silicon Substrates*
15. C. Henkel, S. Abermann, O. Bethge, M. Reiche, E. Bertagnolli, *Process Integration of Pt-Metal-Gate High-k ALD Dielectrics on sSOI*
16. C. Simbrunner, G. Hernandez-Sosa, T.Höfler, G.Trimmel, W. Kern, H. Sitter, *Para-Sexiphenyl Based OLED Devices Grown on Light Sensitive Polymer Substrates*

Sensors:

17. S. van den Driesche, M.J. Vellekoop, *A Sensor Concept for Label-Free Cell Analysis*
18. G. Fercher, W. Smetana, M.J. Vellekoop, *Contactless Conductivity Detection in Ceramics Technology for On-Chip Electrophoresis*
19. M. Rosenauer, M.J. Vellekoop, *Optofluidic Elements for On-Chip Sample Analysis*
20. A. Talić, S. Ćerimović, F. Kohl, F. Keplinger, A. Jachimowicz, *Novel Design and Signal Transduction Concepts of Micromachined Flow Sensors*

Performance of Phonon Depopulated Terahertz Quantum Cascade Lasers

Ch. Deutsch[1], A. Benz[1], G. Fasching[1], K. Unterrainer[1], A. M. Andrews[2], P. Klang[2], W. Schrenk[2] and G. Strasser[2]

[1]Photonics Institute and Center for Micro- and Nanostructures, Vienna University of Technology, Gusshausstrasse 29/387, 1040 Vienna, Austria
[2]Institute of Solid-State Electronics and Center for Micro- and Nanostructures, Vienna University of Technology, Floragasse 7/362, 1040 Vienna, Austria

At present quantum cascade lasers (QCLs) are the most promising candidates as semiconductor based sources in the terahertz region. Unlike their ancestors in the mid infrared, which perform quite well at room temperature, these so called terahertz QCLs are still limited to cryogenic temperatures. The best design so far tops out at 178 K [1].To improve the active region design in these lasers even further one needs to have a profound transport theory including various scattering mechanisms, resonant tunneling and decoherence effects. In collaboration with Prof. Vogl's group from the Walter Schottky Institute we realized a design, which was optimized by employing a Non-equilibrium Green's Functions model [2].

Our active region design is based on the phonon depopulation scheme with a modified doping density to lower the threshold current [3]. Grown by molecular beam epitaxy, the final 15 µm thick GaAs/$Al_{0.15}Ga_{0.85}As$ heterostructure is processed into a strongly confining double-metal waveguide. One drawback of this low doping density is the very small dynamic range limited by an early onset of a negative differential resistance (Fig. 1a). Temperature performance, on the other hand, did not degrade. In the improved structure the barrier responsible for the extraction of the electrons after the lasing transition was optimized. This new design shows a considerably improved dynamic range (Fig. 1b), which usually goes hand in hand with temperature performance. However, the maximum operating temperature just increased by a few Kelvin.

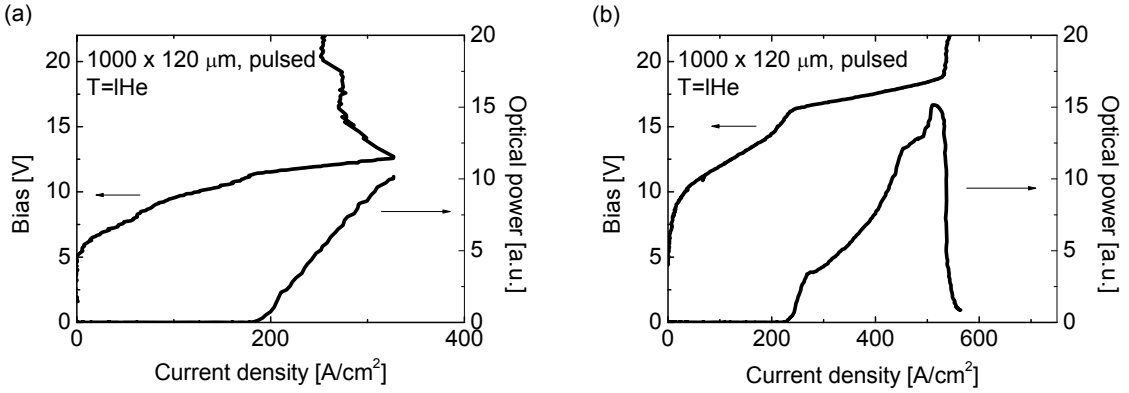

Fig. 1: IV-LI Characteristics. Comparison of the original (a) and the improved (b) structure

Furthermore I will present recent results on devices designed for long wavelength operation reaching frequencies below 2 THz and working up to acceptable temperatures of 105 K.

[1] M. A. Belkin et al, Opt. Exp. 16, 3242 (2008)

[2] T. Kubis et al, J. Comput. Electron. 7, 432 (2008)

[3] A. Benz et al, App. Phys. Lett. 90, 101107 (2007)

Photonic Crystal Frequency Control in Terahertz Lasers

A. Benz[1], Ch. Deutsch[1], G. Fasching[1], K. Unterrainer[1], A. M. Andrews[2], P. Klang[2], W. Schrenk[2] and G. Strasser[2]

[1] Photonics-Institute and Center for Micro- and Nanostructures, Vienna University of Technology, Gusshausstrasse 29/387, A-1040 Vienna, Austria
[2] Institute of Solid State Electronics and Center for Micro- and Nanostructures, Vienna University of Technology, Floragasse 7/362, A-1040 Vienna, Austria

The Terahertz (THz) spectral region is very attractive for applications like spectroscopy, imaging or gas analysis due to the fundamental absorption lines of molecules lying at these energies. All these applications require narrow-band and coherent sources with a precise frequency control. THz quantum-cascade lasers (QCLs) are the preferred sources in this spectral region. Due to their designable gain it is possible to tune the emission from 1.2 to 4.9 THz without changing the material system. However, the inhomogeneously broadened gain leads to multi-mode emission. Therefore, it is necessary to find a way for further frequency control.

Photonic crystals (PhCs) are excellent candidates for the frequency tuning due to their designable dispersion. This allows to precisely control the optical properties of a laser resonator. Our first experiments use a PhC mirror which surrounds the laser gain medium. The PhC has a complete bandgap for TM-polarized light which allows its use as a frequency selective mirror. Thereby, we can shift the emission of our lasers from the gain maximum of the active region into the frequency region where the bandgap mirror has the lowest losses. These devices allow for a simple processing in combination with a reasonable frequency control. Nevertheless, this approach relies on a relative broad bandgap of the PhC which leads typically to a multi-mode emission of the lasers.

The goal is the realization of active PhC lasers. These devices do not rely on a spatial separation of the gain region and the frequency selective mirror but on true PhC-modes. In this scheme the defect free PhC has to provide the optical gain and the feedback at the same time. This allows for a very precise frequency control as these devices now operate in the slow-light region at high symmetry points of the PhC. Our first experiments show that these devices allow for a stable single-mode emission under all driving conditions and a tuning range of 0.4 THz.

Fabrication of Ordered Ge Quantum Island Arrays on Prepatterned SOI Platform for Waveguide Photodetectors and Emitters

Gang Chen, V. Lavchiev, F. Schäffler, G. Bauer, W. Jantsch

Institute of Semiconductor and Solid State Physics, Johannes Kepler University, Linz, Austria

Silicon-on-insulator substrates offer opportunities for integrated optics and micro photonic applications. A thick buried oxide covered by a crystalline silicon layer leads to a very high difference of refractive index, which is as large as two in the near-infrared spectral range. With such a large variation, strong optical confinement can be easily achieved in the transparency window of silicon, and in particular, in the spectral windows around 1.3 and 1.55 μm corresponding to the telecommunication wavelengths. Meanwhile Ge/Si self-assembled islands with their high-Ge content are good candidates to operate at telecommunication wavelengths. And they can be epitaxially covered by silicon and offer the advantage of silicon-terminated surfaces, thus keeping the compatibility with silicon standard processing. Moreover our recent works show the ordered Ge quantum island arrays could be obtained by growth on prepatterned Si substrates. The ordered Ge quantum island arrays could provide high homogeneity in both size and height of the Ge islands, which might lead to the narrowing of the photo emission.

In this work, we report on the fabrication of a set of ordered Ge self-assembled quantum dots arrays on a prepatterned SOI platform. Structural and optical, as well as electronical analysis of the arrays is presented.

Highly Efficient (Infra)-Red-Conversion of InGaN Light Emitting Diodes by Nanocrystals, Enhanced by Color Selective Mirrors

R. Seyrkammer, J. Roither , M.V. Kovalenko and W. Heiss

Institute of Semiconductor and Solid State Physics, University of Linz, Altenbergerstraße 69, 4040 Linz, Austria

The high quantum yield and environmental stability of colloidal nanocrystals, together with their high flexibility in terms of emission wavelength tuning and processability [1] makes them very favorable as nano-phosphors. White light is commercially obtained from light emitting diodes based on III-V nitride compound semiconductors by color conversion with cerium-based phosphors. The resulting color rendering index is, however, rather moderate in the low color-temperature region. To compensate this shortcoming, novel phosphor materials emitting in the red such as Eu_{2+}-doped ternary nitrides or organic materials are discussed. As an alternative nano-phosphor, we introduce colloidal nanocrystals. In particular, nanocrystal-polymer blends are deposited in form of films onto the enclosure of commercial InGaN light emitting diodes to operate as precisely color-tunable nano-phosphors for color conversion with high color stability. Dependent on the choice of the nanocrystal materials, either CdSe/ZnS or PbS nanocrystals are applied, the diode emission is converted to the red or to infrared light, with similar quantum efficiencies. The color conversion is further improved by dielectric mirrors with high reflectivity at the emission band of the nanocrystals, resulting in an almost doubling of the nanocrystal light extraction from the devices, which increases the nanocrystal device efficiency up to 19.1%.

[1] J Lee, V C Sundar, J R Heine, M G Bawendi, and K F Jensen, Adv. Mater. 12, 1102 (2000).

Widely Tunable and Intense Mid-Infrared PL Emission from Epitaxial Pb(Sr)Te Quantum Dots in a CdTe Matrix

S. Kriechbaumer[1], T. Schwarzl[1], H. Groiss[1], W. Heiss[1], T. Wojtowicz[2], G. Springholz[1]

[1] Institute of Semiconductor Physics, Johannes Kepler Universität, Linz, Austria
[2] Institute of Physics, Polish Academy of Sciences, Warsaw, Poland

PbTe belongs to the narrow gap lead-salts giving emission in the mid-infrared (MIR) and exhibiting nearly symmetric conduction- and valence bands and small Auger recombination rates. Therefore, PbTe is well suited for the fabrication of MIR optoelectronic devices. For such devices, quantum dot (QD) active regions would be desirable. Lead salt QDs are typically fabricated as colloidal nanocrystals giving strong emission between 1 – 4 µm. Also, MBE grown Stranski-Krastanow (SK) PbSe QDs were successfully prepared; however, these dots suffer from a strain-induced type-II band alignment.

Recently, we have demonstrated a completely different approach for the synthesis of epitaxial QDs. It is based on phase separation between two lattice-*type* mismatched, immiscible materials, i.e., PbTe (rock salt) and CdTe (zinc blende). Upon thermal annealing, MBE grown 2D PbTe layers within CdTe barriers are transformed into PbTe QD nano-precipitates with highly symmetric almost spherical shapes and atomically sharp hetero-interfaces. These QDs exhibit a large quantum confinement (ΔE_g(PbTe-CdTe) = 1.2 eV) and show intense continuous-wave (cw) PL even at room temperature [1], [2].

In this work, we report the growth of Pb(Sr)Te dots carried out in a IV-VI / II-VI MBE system. In contrast to our earlier work several µm thick CdTe buffer layers, on GaAs (100) substrates without additional MnTe layers were used which yield high quality Pb(Sr)Te dots as evidenced by TEM and cw-PL. In detail, we demonstrate for the first time $Pb_{0.93}Sr_{0.07}Te$ ternary QDs also giving strong PL emission at room temperature. Due to the increasing band gap with increasing Sr content, this leads to a larger tunability of the emission towards shorter wavelengths. Remarkably, for originally 1 nm thin PbSrTe layers, the PL signal is much stronger as compared to a 1 nm PbTe reference dot sample, despite the shorter emission wavelength for the PbSrTe sample. We also observed for thin PbSrTe layers that the blue shift with regard to the bulk band gap is much lower as expected indicating that part of the Sr is incorporated in the CdTe matrix material.

Furthermore, we show that it is possible to fabricate high quality PbTe dots by simply growing 50 – 300 nm thick ternary $Cd_{1-x}Pb_xTe$ layers with Pb-contents of 1% to 6%. The strong PL emission at room temperature is peaked at about 2 – 2.3 µm indicating a rather small average dot size of 9 – 11 nm in diameter depending on the actual Pb content. Recently, we showed that the size of the PbTe dots can effectively be tuned by the original 2D PbTe layer thickness [3]. In addition to that, we demonstrate here that size control is also obtained for a fixed layer thickness by variation of the growth temperature. For a nominally 1 nm PbTe layer, dots with average diameter of 10 nm for 300 °C and of 15 nm for 400 °C growth temperature are found.

[1] W. Heiss, H. Groiss, E. Kaufmann, G. Hesser, M. Böberl, G. Springholz, F. Schäffler, K. Koike, H. Harada, M. Yano, Appl. Phys. Lett. **88**, 192109 (2006).

[2] W. Heiss, H. Groiss, E. Kaufmann, G. Hesser, M. Böberl, G. Springholz, F. Schäffler, R. Leitsmann, F. Bechstedt, K. Koike, et al., J. Appl. Phys. **101**, 081723 (2007).

[3] H. Groiss et al., Appl. Phys. Lett. **91**, 222106 (2007)

Coupled Surface States in Thin, Frequency Dependent Layers

M. Bergmair and K. Hingerl

CD-Labor für oberflächenoptische Methoden, Institut für Halbleiter- und Festkörperphysik, Johannes Kepler Universtät Linz, 4040 Linz;

A negative dielectric function of e.g. a metal allows to excite surface plasmons (SP) along the interface of the metal and a positive dielectric material. The dispersion is derived by using continuity of the fields and reads $k_y = \omega(e_b\, e(\omega)/(e_b+e(\omega))^{1/2}$ [1]. Here, k_y is the wave vector component which is parallel to the interface, e_b the positive dielectric material (we use air with $e_b = 1$) and $e(\omega)$ the frequency dependent dielectric function of the metal (as a first approximation we use the Drude model including damping). The resulting dispersion is below the light line and therefore one has to use e.g. a grating or a prism to excite SPs.

The above solution for SPs at one interface is obtained by the given analytic equation. The next step is to study the coupling of SPs on parallel interfaces. Therefore we derive the two resulting modes (symmetric and antisymmetric mode) at a thin metallic sheet [2]. The dispersion is obtained from an implicit equation [3] and reads $e(\omega)\, k_b /(e_b\, k_m) = \tan(k_m\, d/2)^{\pm 1}$ where $k_i = (k_y^2 - e_i\, \omega^2)^{1/2}$ and d the thickness of the metallic sheet. It is suggested in literature [4] to solve this equation numerically by the Nelder-Mead minimization algorithm [5]. This algorithm works for minimization in arbitrary dimensions (we have a two dimensional minimization: $\mathrm{Re}(k_y)$ and $\mathrm{Im}(k_y)$).

For a single thin film one solution is hardly damped, the dispersion is very close to the light line below the asymptotic frequency and this asymptotic frequency shifts towards the plasma frequency of the metal as the thickness is decreased. The second solution is strongly damped and lies well below the light line.

In our contribution we investigate the coupling of surface plasmons over adjacent layers and therefore follow the derivation given in [2]. For each thin film one obtains two more solutions which are degenerate for large distances between the layers (or thick films). We study the coupling by means of the Nelder-Mead algorithm, investigate the influence of the geometry (distance between the metallic layers and their thickness) and give the dispersion of surface plasmons in a photonic crystal.

The authors would like to thank two EC grants (N2T2 and NanoCharM).

[1] H. Raether, Surface Plasmons on Smooth and Rough Surfaces and on Grantings. Springer, Berlin, 1988.

[2] E. N. Economou, Phys. Rev., vol. 182, pp. 539 Jun 1969.

[3] A. Zayats, I. Smolyaninov, and A. Maradudin, Physics Reports, vol. 408, pp. 131 2005.

[4] J. Dionne, L. Sweatlock, H. Atwater, and A. Polman, Physical Review B, vol. 72, p. 075405, 2005.

[5] J. Nelder and R. Mead, The Computer Journal, vol. 7, p. 308, 1964.

Intraband Auger Effect in InAs/InGaAlAs/InP Quantum Dot Structures

T. Gebhard[1], D. Alvarenga[2], P. L. Souza[3], P. S. S. Guimarães[2], K. Unterrainer[1], M. P. Pires[4], G. S. Vieira[5], J. M. Villas-Boas[2,5] and N. Studart[6]

[1]Photonics Institute, Technische Universität-Wien, A-1040 Vienna, Austria
[2]Departamento de Física, Universidade Federal de Minas Gerais, 30123-970, Belo Horizonte, Brazil
[3]LabSem/CETUC, Pontifícia Universidade Católica, Rio de Janeiro, 22451-900, Brazil
[4]Instituto de Física, Universidade Federal do Rio de Janeiro, 21945-970, Rio de Janeiro, Brazil
[5]Divisão de Física Aplicada, Instituto de Estudos Avançados, 12228-001, São José dos Campos, Brazil
[6]Departamento de Física, Universidade Federal de São Carlos, 13565-905, São Carlos, Brazil

A theoretical study in the 90's showed that inter- and intraband Auger scattering in quantum dots are very effective processes [1]. The activation of photoexcited electrons by Auger scattering in interband transitions has been shown experimentally for InAs/InP QD structures [2]. However, experimental evidence of the Auger effect on intraband transitions has not been reported yet. In this work we present results that suggest that Auger processes play a fundamental role in generating an intraband PC.

InAs QDs with different doping levels were deposited by metalorganic vapor phase epitaxy on 100 nm InGaAlAs layers lattice-matched to InP with 18% Al content and covered by a 13 nm thick InP barrier. Ten periods of the dot structure were grown between *n* doped contact layers. A QD density and height of 1.2×10^{10} cm^2 and 9 nm, respectively, were determined by atomic force microscopy measurements. Transmission electron microscopy images showed lens shaped QDs.

According to theoretical calculations using a 3D effective mass approximation model assuming cylindrical symmetry [3], the strongest absorption is expected to occur between the ground state and the fourth excited state at an energy of 187 meV. Intraband PC measurements show a peak at 190 meV, even though these states are about 200 meV from the continuum. The quaternary material barriers are 100 nm thick. This makes a tunneling mechanism unlikely under flat band conditions. Absorption at this energy has been observed on contactless equivalent samples with 20 periods. The PC has been measured as a function of temperature without applied bias voltage.

Nearly no temperature dependence was observed on the PC signal up to 60K. That leads to the conclusion that the photo-excited electrons don't get activated by a thermal process. This is strong evidence for Auger scattering where one electron relaxes inside or into a QD transferring its energy to the electron on the final state of the absorption to allow for this electron to contribute to the PC. The latter is, in turn, promoted to energies above the quaternary material band edge, where it can contribute to the current.

The results obtained indicate that quantum dot photodetector structures can, in principle, be designed to operate based on the more selective bound-to-bound transitions of quantum dots and still produce an efficient device.

[1] J. L. Pan, Phys Rev. B 49, 11272 (1994).

[2] L. Landin *et al*, J. Appl. Phys. 95, 8007 (2004).

[3] P. L. Souza *et al*, Appl. Phys. Lett. 90, 173510 (2007).

Quantitative Scanning Capacitance Microscopy on Buried InAs Quantum Dots

J. Smoliner, W. Brezna, A.M. Andrews, G. Strasser

Institut für Festkörperelektronik, TU-Wien
Floragasse 7, A-1040 Wien, Austria

InAs self assembled quantum dots embedded in GaAs *n* − *i*−Schottky diodes were imaged by quantitative scanning capacitance microscopy. As these measurements are extremely sensitive to light, a modified AFM feedback procedure was developed, where the AFM laser can be turned off up to several seconds while the AFM feedback loop keeps running.

The InAs quantum dot samples we used for our capacitance studies were initially designed for photocurrent spectroscopy, and had the following layer structure: on a highly doped *n*-doped back contact, a 40 nm i-GaAs layer was grown. On top, 1.55 ML of InAs were deposited at 500 °C followed by 80 nm of *i*-GaAs, a 40 nm thick AlGaAs blocking barrier (Al concentration 30%), and a 10 nm GaAs capping layer. The nominal dot density was in the order of 500 μm^{-2}.

In the low frequency (f = 1 kHz) capacitance images, InAs dots are clearly visible. The dot size in the capacitance images is larger compared to what was expected for the geometrical size, which we attribute to the fact that the dots are located 130 nm below the sample surface. A contrast rich capacitance landscape is also revealed in between the dots, which we attribute to local thickness variations of the InAs wetting layer. We also find that the image contrast depends on sample bias. A systematical measurement yielded best contrast at a sample bias of –0.6 V, which approximately corresponds to flatband conditions.

In addition to the images, capacitance spectra were recorded at on-dot and off-dot positions, which exhibit a clearly different behavior. At off-dot positions, the capacitance increases monotonically in forward bias direction, as it is expected for the capacitance of a Schottky contact on semiconductors. On contrast to that, one clear minimum and a step-like feature is observed in the capacitance spectra at on-dot positions. Attributing these features to a sequential filling of the dot states, the level spacing can be determined. For our sample, we obtain an energy spacing of 46 meV between the lowest levels, which is in reasonably good agreement with previous results of optical measurements.

Characterization of Nanowires

M. Keplinger[1], D. Kriegner[1], B. Mandl[1, 2], J. Stangl[1], V. Chamard[3], E. Wintersberger[1], R.T. Lechner[1], D. Hufnagl[1] and G. Bauer[1]

[1]Institut für Halbleiter- und Festkörperphysik, Johannes Kepler Universität Linz, Altenbergerstrasse 69, 4040 Linz, Austria
[2]Solid State Physics, Lund University, Professorsgatan 1, 22100 Lund, Sweden
[3]Université P. Cezanne Aix-Marseille III, CEDEX 20, 13397 Marseille, France

Nanowires have become of great interest in the recent years, due to their unique electronical and structural properties. Such structures provide one-dimensional electronic material and the possibility to connect single quantum dots, which are zero-dimensional electronic structures. In addition, nanowires exhibit interesting mechanical properties which make new, so far not studied, combinations of materials possible. The most significant demonstration of this possibility is the growth of III-V nanowires on Si substrates [1, 2]. Since such structures are interesting for fundamental science as well as for applications, a thorough study of the material properties and the material quality is needed.

We show x-ray techniques for material studies of nanowires, to investigate epitaxial orientation of the wires, material composition, and crystal structure (zinc-blende, wurtzite) of nanowires:

- Deriving the P-concentration of $InAs_{1-x}P_x$ by high-angle x-ray diffraction:
  A sample series of $InAs_{1-x}P_x$ nanowires, grown using a gold-free nucleation process, was investigated by recording asymmetric reciprocal space maps with our Seifert XRD 3003 laboratory source, to give feedback on P incorporation to the sample growers.
- Obtaining the orientation of epitaxial InP nanowires using grazing incidence angle diffraction (GID):
  Due to a low diffraction intensity from the substrate, GID is very beneficial for the measurement of nanowires. Recorded reciprocal space maps clearly show streaks of the hexagonal wire side facets.
- Wurtzite to zinc-blende ratio in wire ensembles:
  By comparing (10–1.0), (20–2.0), and (30–3.0) hexagonal GID intensities with their theoretical values, we derive the wurtzite concentration in measured wire ensembles: although bulk InAs crystallizes in cubic zinc-blende lattice structure, in thin InAs nanowires a considerable fraction of hexagonal wurtzite lattice is found.
- Studies of single nanowires have so far only been made by transmission electron microscopy, using focused beam and coherent scattering, x-ray diffraction has now been successfully applied [3].

[1] B. Mandl, J. Stangl, T. Martensson, A. Mikkelsen, J. Eriksson, L. S. Karisson, G. Bauer, L. Samuelson, and W. Seifert, Nano Letters 6, 1817 (2006).

[2] T. Martensson, J. B. Wagner, E. Hilner, A. Mikkelsen, C. Thelander, J. Stangl, B. J. Ohlsson, A. Gustafsson, E. Lundgren, L. Samuelson, et al., Advanced Materials 19, 1801 (2007).

[3] V. Chamard, J. Stangl, S. Labat, B. Mandl, R. T. Lechner, and T. H. Metzger, J. Appl. Cryst. 41, 272 (2008).

Low Dimensional Nanostructures Grown by Molecular Beam Epitaxy

P. Klang, H. Detz, A.M. Andrews, B. Basnar, W. Schrenk, A. Lugstein and G. Strasser

Center for Micro- and Nanostructures, Vienna University of Technology, Floragasse 7, Vienna, Austria
Institute for Solid State Electronics, Vienna University of Technology, Floragasse 7, Vienna, Austria

Self-assembled semiconductor quantum dots (0D system) have attracted researchers for more than 20 years because of their unique electronic and optoelectronic properties based on reduced dimensionality. In the last several years 1-D nanowires are entering the field of nanoscaled devices. We present the growth and characterization of these low dimensional structures grown by solid source molecular beam epitaxy (MBE) system.

For the 0-D structures, we focus on the growth of high quality InAs quantum dots (QDs) in $Al_xGa_{1-x}As$ matrix for prospective incorporation into intersubband devices like MIR detectors, THz detectors and quantum cascade lasers (QCLs). The growth temperature, growth rate and deposited InAs layer thickness are key parameters to control QD energy levels. For QCLs based on GaAs/$Al_xGa_{1-x}As$ material we need the QD ground state energy above GaAs conduction band edge and a narrow size distribution of the QDs. Photoluminescence measurements were performed to obtain the QD ground state energy. To decouple the density and size of the QDs we use a low InAs growth rate of 0.01 µm/h. At this low growth rate the density depends mainly on the growth temperature and size of QDs is controlled by the deposited InAs thickness. The Al content of the embedding material also influences the QD properties. For a higher Al concentration the QD density is increased while the QDs size is reduced. QDs grown on $Al_xGa_{1-x}As$ surfaces have also higher inhomogeneous size distribution. The QD size and density were obtained by atomic force microscopy measurements of surface dots. We have improved the QD size distribution by lowering the As_4 flux during the InAs growth.

We also study the MBE growth of III-V self-assembled one-dimensional nanowires on Si nanowires grown by low-pressure chemical vapor deposition. To understand the growth mechanism, GaAs growth rates were varied from 0.1 – 0.5 µm/h and various III/V ratios were used to deposit equivalent layer thicknesses ranging from 40 – 200 nm. Additionally, we investigated MBE growth of GaAs nanowires on different Si substrates with Au catalysts and with various pre-growth surface treatments using buffered HF. The samples were analyzed by scanning electron microscopy, photoluminescence measurements, high resolution transmission electron microscopy and x-ray diffraction analysis.

Recent Improvements on InAlN/GaN MOS-HEMTs

G. Pozzovivo[1], J. Kuzmik[1,2], S. Abermann[1], C. Ostermaier[1], J.-F. Carlin[4], M. Gonschorek[4], E. Feltin[4], J. Liday[3], N. Grandjean[4], E. Bertagnolli[1], G. Strasser[1] and D. Pogany[1]

[1] Institute of Solid-State Electronics, Vienna University of Technology, Vienna, Austria.
[2] Slovak Academy of Sciences, Bratislava, Slovakia
[3] Department of Microelectronics, University of Technology, Bratislava, Slovakia
[4] Institute of Quantum Electronics and Photonics, Ecole Polytechnique Fédérale de Lausanne (EPFL), Laussane, Switzerland

Gallium Nitride (GaN) has become the superior material of high power devices in microwave applications due to its large bandgap, the high saturation velocity, the high thermal conductivity, and its high mobility in 2-dimensional electron gas (2DEG). This 2DEG is based on the strong ionic bonding of the GaN crystal structure causing large spontaneous and piezoelectric polarization fields at interfaces [1] as used in conventional AlGaN/GaN high mobility electron transistors (HEMTs). However, the stress at the interfaces limits the device performance. Heterostructure devices based on InAlN/GaN [2] have already shown superior results [3], [4] in comparison to conventional AlGaN/GaN HEMTs, due to their higher spontaneous polarization and the possibility of lattice-matched growth of InAlN on GaN at an indium composition of around 18%. Therefore, higher power operation and thermal stability are expected from such devices. However, RF dispersion defined as decreasing output power at large signal gate modulation is still an important issue to be solved. Preview results on AlGaN/GaN devices have shown that surface-related traps are causing transients that prevent the gate from opening after channel depletion [5], [6].

In this report we present our current improvements on InAlN/AlN/GaN MOSHEMT devices with ZrO_2 or HfO_2 for gate insulation and surface passivation. The lattice-matched heterostructure was grown by metal-organic vapor deposition on sapphire substrate. The 1.1-nm-thick AlN interlayer was inserted in the conventional structure to increase the mobility in the 2DEG. The dielectric deposition was directly done after Ar-based mesa isolation, requiring that post processed steps are done at lower temperatures without dielectric degradation. It was found out that plasma pre-treatment with $SiCl_4$ before metal evaporation could decrease the ohmic resistance to 0.7 Ohm/mm after annealing at only 600 °C. Investigating the surface by Auger electron spectroscopy (AES) showed that the total concentration of carbon impurities was reduced only after pre-treatment and for lower temperatures. The final gate processing was done by 2 µm wide Ni/Au contacts.

The gate leakage current for the insulated devices was reduced by more than three orders of magnitude compared to the Schottky-barrier (SB) HEMT below 1 µA/mm. The output characteristic of the MOS-HEMT was not only improved by higher drain current at increased forward bias, possible due to the gate insulation, but also showed slightly higher transconductance g_{me} than the compared SB HEMT. This behavior was explained by improvement of the intrinsic mobility below the gate, which is more effective in long channel devices [7]. Additionally, no RF dispersion occurred in ZrO_2- and HfO_2-based MOS-HEMT in contrast to the non-passivated SB HEMT.

[1] O. Ambacher et al., J. Appl. Phys., vol. 85, pp. 3222–3233, 1999
[2] J. Kuzmik, IEEE Electron Device Lett., vol. 22, no. 11, pp. 510–512, 2001.
[3] J. Kuzmik et al., IEEE Transactions on Electron Devices, vol. 55, no. 3, 2008
[4] F. Medjdoub et al., 2006 Int.Electron Devices Meeting (IEDM), 2006, Tech. Digest, 927
[5] R. Vetury, IEEE Transactions on Electron Devices, vol.. 48, no. 3, 2001
[6] E. Kohn et al., IEEE Trans. on Microwave Theory and Techniques, vol. 51, no. 2, 2003
[7] G. Pozzovivo et al., Applied Physics Letters, vol. 91 (4), 043509, 2007

Voltage Tunability of Intersubband Lifetimes in SiGe Quantum Well Structures

P. Rauter[1], T. Fromherz[1], G. Bauer[1], N.Q.Vinh[2], G. Mussler[3], D. Grützmacher[3]

[1]Institute for Semiconductor and Solid State Physics, Johannes-Kepler-University Linz, Austria
[2]FOM Institute for Plasma Physics Rijnhuizen, Nieuwegein, Netherlands
[3]Institut für Bio- und Nanosysteme, Forschungszentrum Jülich, Jülich, Germany

Driven by the strong need for Si-based optoelectronic devices for a wide range of applications, considerable endeavors have been made to develop a laser in this material system. Silicon is an indirect semiconductor and therefore cannot be used for direct optical transitions over the bandgap. However, the concept of infrared emitters based on quantum cascade heterostructures, which is very successfully applied to III-V material systems, constitutes a promising approach towards a SiGe infrared laser. But while emission of infrared radiation of various wavelengths has been demonstrated for p-type SiGe quantum cascade structures [1] [2], lasing has yet to be achieved.

One of the key issues for the achievement of lasing is the build up of population inversion, which is essentially dependent on the excited state's lifetime. As valence band structure calculations for SiGe heterostructures are of high complexity, it is crucial to acquire the key intersubband relaxation times experimentally. In previous works we reported the first direct determination of ultrashort HH2-HH1 relaxation times (550 fs) by pump-pump photocurrent experiments [3] and compared transmission pump-probe experiments with pump-probe PC measurements by determining SiGe LH1-HH1 relaxation times in the ps regime, pointing out the advantage of latter [4].

In the course of this work we have designed and grown SiGe quantum well structures, for which it is possible to shift the center of the first excited hole state (LH1) from a central quantum well into a shallow side well by changing the bias at the sample contacts. It is thus possible to change the transition between LH1 and HH1 from a locally direct to an indirect one by varying the sample bias, inducing an alteration of the lifetime of the first excited LH1 state. In order to investigate the sample's relaxation behavior, we have performed pump-pump measurements using the free electron laser FELIX at the FOM, Nieuwegen. The FEL wavelength was tuned to 41.3 µm in order to be in resonance with the HH1-LH1 transition of the central well. The photocurrent through the sample was measured as a function of the delay between two pump-micropulses, whose polarizations differed by 90°. The first laser pulse populates the LH1 state, while the second excites carriers from this state into the continuum, where current is possible. As the HH1-LH1 transition is only allowed in TE polarization, the gained signal curve is asymmetric in respect to the sign of the delay between the TM and TE pulses. The PC decay was measured for a series of bias voltages, and a clear change in the long decay of the PC signal between 13 ps and 20 ps could be observed for a bias variation from 0.3 to 2 V. Thus we can report a significant tunability of the excited state lifetimes of SiGe quantum wells by the applied voltage.

[1] G. Dehlinger et al., Science **270**, 2277 (2000)

[2] S.A. Lynch et al., Material Science and Engineering B **89**, 10 (2002)

[3] P. Rauter et al., Applied Physics Letters **89**, 211111 (2006)

[4] P. Rauter et al., New Journal of Physics **9**, 128 (2007)

In-situ STM Studies of Ge Growth on Stripe-Patterned Si-(001)

D.G. Matei, B. Sandujav, G. Chen, F. Schäffler and G. Springholz

Institut für Halbleiterphysik, Johannes Kepler University, A-404 Linz, Austria

Self-organized ordered Ge-island growth on pre-patterned Si substrates has attracted great interest for controlled positioning of quantum dots in nano-electronic devices. The growth on pre-patterned substrates is rather complex due to the complicated morphological evolution of the growth surface [1] – [3]. In this work, scanning tunneling microscopy was used to investigate Si and Ge growth on stripe patterned Si substrates with high resolution, focusing in particular on the role of the stripe orientation relative to the in-plane [110] direction.

Si (001) substrates were stripe patterned using e-beam lithography and reactive ion etching. Stripes with different widths were obtained by changing the e-beam exposure dose. For Si buffer layer, a two-step growth procedure was employed, consisting of 35 nm deposition at 450 °C followed by 15 – 20 nm at 520 °C. After patterning, the stripes have a rectangular cross-section. During buffer growth, Si atoms diffuse to the areas with the highest curvature, causing an increasing rounding of the grooves. As a result, the stripes are transformed to a "U"-shaped geometry, with sidewalls composed of various metastable Si {11n} facets, with inclination ranging from 7.3 – 25°. With further growth, the steep middle part of the side walls narrows, leading to a "V"-shaped geometry with 8-10° inclination. Stripes with different widths also show different profiles at the same buffer thickness. For the differently oriented stripes, the dimer row direction changes with respect to the stripe orientation. This strongly affects Si-adatom diffusion. Thus, the grooves are filled up much more rapidly, i.e., the transition from rectangular to V-shaped profiles occurs earlier. Even more, on such stripes the side walls cannot develop the characteristic {11n} facets, leading to a side wall corrugation, characterized by {11n} micro facets separated by pronounced step bunches.

Ge growth on top of the buffer layers was interrupted at different stages for STM investigations. Initially, on the stripes oriented along [110] Ge produces {105} facetted surface ripples with an average width of 17 nm on the sidewall segments with 8° inclination. On the stripes oriented between [110] and [100] directions, the corrugated sidewalls are converted also into regularly spaced, but asymmetric {105}-faceted ripples. For the particular case of stripes oriented along [100], the rough sidewalls, obtained after Si buffer, are transformed into large, flat {105} surfaces. Dot nucleation, occurring after the growth of additional Ge layers, is observed to take place at the concave intersections between various facets seen after the growth of silicon buffer. For U-shaped grooves, dots nucleate somewhere in the middle of the sidewalls and have an asymmetric shape due to the local inclination of the base plane. On V- or truncated V-shaped grooves, the concave intersections are found at their bottom for the former case, or between the bottom and sidewalls for the latter. This is better observed for the stripes which have a closer orientation to [100].

[1] C. Dais, H.H. Solak, Z. Ekinci, D. Gruetzmacher Surf. Sci., 601, 2787 (2007).

[2] G. Chen, H. Lichtenberger, F. Schäffler, G. Bauer, W. Jantsch Mat. Sci. Eng. C26, 795 (2006).

[3] Z. Zhong, A. Halilovic, M. Mühlberger, F. Schäffler, G. Bauer J. Appl. Phys., 93, 6258 (2003).

Atomic Layer Deposition of High-*k* Gate Dielectrics on Germanium and Silicon Substrates

O. Bethge[1], S. Abermann[1], Ch. Henkel[1], Ch. Straif[2] and E. Bertagnolli[1]

[1]Institute for Solid State Electronics, Vienna University of Technology, Floragasse 7, 1040 Vienna, Austria

[2]Institut für Chemische Technologien und Analytik, Vienna University of Technology, Getreidemarkt 9, 1060 Vienna, Austria

In silicon-based metal oxide semiconductor (MOS) devices a shrinking of the thickness of the gate dielectric is crucial to enable further lateral downscaling of these devices while maintaining proper electrical behavior. Below 1 nm, silicon dioxide dielectrics suffer from high tunnel currents, thus alternative dielectrics must be considered. However, in order to maintain a reasonable drive current level at larger tunnel barrier widths, the permittivity of the new dielectrics have to be a multiple of that of silicon dioxide [1]. Since the native-oxide-route has to be abandoned even for silicon, other semiconductors are entering the arena.

Aside from silicon, germanium (Ge) is an attractive material in downscaled MOS devices due to its high electron mobility and its low dopant activation temperatures. The fact that Ge is not offering a stable natural oxide is no more a disadvantage over silicon.

For the extrinsic ultra thin dielectric layers envisaged for future CMOS-devices, Atomic Layer Deposition (ALD) is the favored deposition process for high-k dielectric materials like hafnium dioxide (HfO_2) or zirconium dioxide (ZrO_2), due to the high uniformity, high conformity, and the excellent thickness control of the deposited layers [2].

For the deposition process, alternative semiconductors as well as novel device architectures issues a lowering of the deposition temperature well below 300°C is valuable. Furthermore, a low-temperature ALD process may offer the opportunity to incorporate lift-off schemes based on resist polymers [3].

In this paper we deposit high-k-dielectric stacks by ALD on well pretreated Ge and Si surfaces at deposition temperatures ranging from 150°C to 110°C and compare them with dielectrics deposited at the usual higher temperatures ranging from 300°C to 200°C.

By investigating their leakage current and capacitance-voltage characteristics, we have to conclude that at a deposition temperature of about 150°C, electrically superior dielectrics can be grown, thus enabling FET on Si and Ge.

This work is funded by the Austrian Science Fund (FWF), project No. P19787-N14. The support of the GMe, and the Centre for Micro- and Nanostructures, ZMNS is greatfully acknowledged.

[1] Internat. Tech. Roadmap for Semicond. (ITRS), 2007. [http://www.itrs.net/]

[2] T. Suntola, Mater. Sci. Rep. 4 (1989) 261.

[3] M. Biercuk et.al., Appl. Phys. Lett. 83 (2003) 2405.

Process Integration of Pt-Metal-Gate High-k ALD Dielectrics on sSOI

C. Henkel[1], S. Abermann[1], O. Bethge[1], M. Reiche[2] and E. Bertagnolli[1]

[1] *Institute for Solid-State Electronics, TU-Vienna, Floragasse 7, A-1040 Vienna, Austria*
[2] *Max-Planck-Institute for Microstructure physics, Weinberg 2, D-06120 Halle, Germany*

The superior properties of the silicon-silicon dioxide combination are the key to the success and the opportunity to continuously shrink the device geometry of modern transistors. However, to keep the inversion channel in a quasi-2-dimensional arrangement, the silicon dioxide has to be shrunk accordingly to the lateral dimensions. Thus modern devices approach the tunnel limit for the gate dielectric, giving rise to the onset of high gate leakage currents. Silicon dioxide has therefore to be replaced by proper high-k-dielectrics, enabling larger tunnel barriers at approximately the same drive current. In industrial CMOS, such high-k-dielectrics were introduced at and beyond the 45 nm technology node, often in combination with metal gates.

Further improvement of the device performance is addressed by the replacement of bulk silicon as substrate material. By this step, mobility constrains of the bulk silicon substrates should be overcome. Promising candidates for this purpose are high-carrier-mobility substrates like SiGe or Ge. Another approach is the use of engineered substrates like strained silicon, offering the opportunity of an enhancement of both, the electron and the hole mobility [1].

In this presentation we focus on the electrical properties of high-k-dielectric gate stacks, zirconium-oxide (ZrO_2), aluminum-oxide (Al_2O_3) and the mixed oxide lanthanum-zirconium-oxide ($La_xZr_{1-x}O_2$) on strained silicon-on-insulator (sSOI). In order to get both, stoichiometry as well as atomic scale smoothness, these oxides are deposited by Atomic Layer Deposition (ALD) [2]. These properties are compared to those obtained for MOSFET-devices on bulk silicon.

[1] M. Reiche et al., *ECS Transactions*, **6**, 339 (2007)

[2] M. Leskelä and M. Ritala, *Angew. Chem. Int. Ed*., **42**, 1924 (2003).

Para-Sexiphenyl Based OLED Devices Grown on Light Sensitive Polymer Substrates

C. Simbrunner[1], G. Hernandez-Sosa[1], T. Höfler[2], G. Trimmel[2], W. Kern[2,3] and H. Sitter[1]

[1] Institute for Semiconductors and Solid State Physics, Johannes Kepler University Linz, Altenbergerstrasse 69, 4040 Linz, Austria
[2] Institute for Chemistry and Technology of Organic Materials, Graz University of Technology, Stremayrgasse 16, A-8010 Graz
[3] Departement of Chemistry of Polymeric Materials, Franz-Josef-Straße 18, A-8700 Leoben

During the last years organic devices became of increasing interest in many fields of electronics. A bright future for organic light emitting devices (OLED) is expected as organics provide a wide spectrum of molecules emitting at various photon energies [1]. Para-sexiphenyl represents an organic molecule which has been established as active material for blue emitting OLEDs [2], [3].

We report on OLEDs based on Para-sexiphenyl (PSP), which has been deposited by Hot Wall Epitaxy (HWE) on Polynorbornene, a photosensitive polymer. The used substrates have been pre-patterned by UV illumination leading to a changed surface polarity [4] and consequently to an induced change of morphology and crystalline properties of the grown PHP [5]. In particular we report on the optical properties of the devices which can be tuned by UV illumination of the polynorborene substrates.

[1] M. Muccini, Nature materials 5 (2006), 605

[2] G. Kranzelbinder et al., Synthetic Metals 102 (1999), 1073-1074

[3] A. Niko et al., J. Appl. Phys. 82 (1997), 4177

[4] T. Höfler et al., Polymer 48 (2007), 1930-1939

[5] G. Hernandez-Sosa, EMRS abstract, 2008

A Sensor Concept for Label-Free Cell Analysis

S. van den Driesche and M.J. Vellekoop

Institute of Sensor and Actuator Systems, Vienna University of Technology, Vienna, Austria

Contactless Conductivity Detection in Ceramics Technology for On-Chip Electrophoresis

G. Fercher[1,2], W. Smetana[1], M.J. Vellekoop[1]

[1] *Institute of Sensor and Actuator Systems, TU Wien, Austria*
[2] *IMA GmbH, Wiener Neustadt, Austria*

This work reports on a capacitively coupled contactless conductivity detector produced in Low Temperature Co-fired Ceramic (LTCC) technology for microchip capillary electrophoresis (CE). Two measurement electrodes located outside the measurement channel at opposite sides serve as detector, avoiding direct contact with the fluid-filled separation channel. Impedance variations caused by separated ionic species are so measured without galvanic contact of electrodes and fluid. Using the capacitively coupled detector design avoids bubble formation in the channel which impedes the CE process. Furthermore higher electric separation field strengths can be applied as the sensitive detection circuitry is decoupled from the channel. The application of LTCC in combination with contactless conductivity detection is very promising because of its high dielectric constant compared to glass or plastics. This enhances the coupling of the excitation signal into the microfluidic channel and thus results in increased detection sensitivities. Successful separations of three inorganic ions confirm the feasibility of LTCC as a material for on-chip CE when used with contactless conductivity detection.

Optofluidic Elements for On-Chip Sample Analysis

M. Rosenauer and M.J. Vellekoop

Institute of Sensor and Actuator Systems, Vienna University of Technology, 1040 Vienna, Austria

The benefit of the integration of novel optofluidic elements, e.g., fluidic lenses and liquid-core liquid cladding (L2) waveguides, for on-chip optical sample analysis are discussed. In conventional optical miniaturized sensor systems the required measurement sensitivity is achieved by applying extensive and costly source and detection instruments. Using properly designed microfluidic channels, pre-calculated flow rate ratios and transparent fluids with different refractive indices but similar viscosity novel fluidic optical elements can be created. In this contribution we present a dynamically reconfigurable fluidic lens which can focus light three-dimensionally and a L2 waveguide design which can couple the incident laser beam in the analysis channel. Comprehensive finite element simulations of the fluids and ray-tracing simulations of the optical system have shown a numerical relation between flow rates and lens curvature resulting in a variable focal length. The light waveguide chip enables a novel analytic channel excitation technique simplifying the light guidance on the chip. It also reduces the influence of the surface roughness of the fluidic channel sidewalls on the transmission coefficient. Both optofluidic systems are fabricated on a glass substrate in a photosensitive polymer by fast laser micro-stereolithography. We succeeded in manufacturing a single high quality prototype in less than 1.5 hours.

Novel Design and Signal Transduction Concepts of Micromachined Flow Sensors

A. Talić[1], S. Ćerimović[1], F. Kohl[1], F. Keplinger[2], A. Jachimowicz[2]

[1]FISS, Austrian Academy of Sciences, Wiener Neustadt, Austria
[2]ISAS, Vienna University of Technology, Vienna, Austria

A typical calorimetric flow sensor consists of a miniaturized heat source and spatially separated temperature sensors (thermistors), all embedded in a thin membrane. The sensor relies on flow dependent heat transfer altering the temperature distribution near the heater. This change can be converted into an output voltage and evaluated for the determination of essential flow parameters such as flow velocity or mass flow.

In this work we investigate the novel design ideas and signal transduction concepts for micromachined calorimetric flow sensors. Multiples of high-resolution thermistors are placed symmetrically to a thin-film heater on the sensor membrane. Comprehensive finite element analyses revealed that beside the conventional calorimetric transduction such sensors are also operable in a mixed calorimetric-anemometric mode. Based on the self heating effect of the employed high resolution thermistors, this operational mode combines the extremely low power consumption with high flow sensitivity and an unambiguous transduction characteristic over a wide flow range. Moreover, the thermistors are connected to form a Wheatstone bridge. This reduces the complexity of subsequent evaluations circuits, since it can be easily read-out by means of a high-impedance galvanometer.

The use of alternative electronic circuits for the generation of flow signals is also investigated. Maintaining a constant average excess membrane temperature by means of a simple two-state electronic controller, a pulse modulated actuation signal is obtained. The pulse duration and repetition rate are determined by selected amplitude and the dynamic characteristics of the thermal system, which in turn depend on flow velocity. This approach offers the quotient of high to low pulse duration as an output quantity in addition to the temperature difference signal.

For a convenient controller design, we developed a comprehensive SPICE model of the thermal system which fully covers its static and dynamic behavior. The parameters of the on-off controller can be tuned to enable optimum transduction for a specified flow range and by that outperform classical analogue controllers. Experiments confirm that this approach is a convenient method for the development of optimized controllers for any calorimetric flow transducer and specific measurement tasks.